Electric-Field Modulation of Damping Constant in a Ferromagnetic Semiconductor (Ga,Mn)As

Lin Chen,[1] Fumihiro Matsukura,[1,2,3,*] and Hideo Ohno[1,2,3]
[1]WPI-Advanced Institute for Materials Research (WPI-AIMR), Tohoku University, 2-1-1 Katahira, Aoba-ku, Sendai 980-8577, Japan
[2]Center for Spintronics Integrated Systems, Tohoku University, 2-1-1 Katahira, Aoba-ku, Sendai 980-8577, Japan
[3]Laboratory for Nanoelectronics and Spintronics, Research Institute of Electrical Communication, Tohoku University, 2-1-1 Katahira, Aoba-ku, Sendai 980-8577, Japan

(Received 2 December 2014; revised manuscript received 18 May 2015; published 30 July 2015)

The modulation of the Gilbert damping constant α in (Ga,Mn)As by the application of an electric field is detected by ferromagnetic resonance measurements, where α increases with decreasing hole concentration. The smaller modulation of other magnetic parameters, such as magnetic anisotropy fields and Landé g factor, suggests that the modulation of α is governed by other effects rather than the spin-orbit coupling. Comparison of the conductivity dependence of α with that of the magnetization indicates that the magnetic disorder induced by carrier localization plays a major role in determining the magnitude of α in (Ga,Mn)As.

DOI: 10.1103/PhysRevLett.115.057204 PACS numbers: 75.50.Pp, 76.30.-v, 76.50.+g

The Gilbert damping constant α, which determines the relaxation and coherence of collective spins, is one of the fundamental parameters governing the magnetization dynamics in ferromagnets [1]. It is also critical for the performance of spintronics devices, such as for the threshold current for spin-transfer torque switching [2,3]. The damping constant is considered to consist of extrinsic and intrinsic terms. The intrinsic one for metal magnets is known to be related to spin-orbit coupling, density of states at Fermi level, and electron scattering rate [4–6]. The extrinsic one is found in magnetic and nonmagnetic heterostructures, where α of the magnetic layer is enhanced by a nonlocal spin relaxation process in the adjacent nonmagnetic layer [7,8]. To address damping mechanisms, experimental work was carried out on various material systems [9–11]. Some routes for manipulating α were also investigated, such as material engineering [4,5,9–11], size effect [12], spin pumping [7,8], and electric-field effect [13]. While the material dependent nature of α was confirmed, details of the mechanism determining α are yet to be established. Thus, a method for tuning α in the same material by external means is vital to elucidate the mechanism, as well as to search ways to control the magnitude of α [13]. In this Letter, in an effort to shed light on the mechanism, we focus on the electric-field effect on α of a ferromagnetic semiconductor, (Ga,Mn)As. Electric-field control of magnetism is now one of the most important subjects in the field of spintronics, because it is expected to provide an opportunity to develop new functional devices. So far, electric-field effects, such as control of the Curie temperature T_C, magnetic anisotropy, and the coercive force, have been realized in magnetic semiconductors and then in ferromagnetic metals [14–27]. Here, we show that α of (Ga,Mn)As can be modulated by the application of an electric field onto a metal-insulator-semiconductor (MIS) structure. The results show that carrier localization exerts a major influence on the magnetization relaxation in (Ga,Mn)As.

A (Ga,Mn)As film with nominal Mn composition x of 0.13 and thickness of 4 nm is grown at 185 °C on a GaAs (001) substrate by low-temperature molecular-beam epitaxy (MBE) through a buffer layer consisting of 4 nm GaAs and 30 nm $Al_{0.8}Ga_{0.2}As$ [16,28]. After removal from the MBE chamber, the sample is annealed at 200 °C for 10 min in the air to increase conductivity and magnetization [29], which increases T_C from 60 K to 100.6 K. Magnetization measurements reveal that the sample does not include detectable MnAs second phase with $T_C \sim 310$ K. Relatively high Mn doping and post-growth annealing are used to make the sample be in the metallic side of the metal-insulator transition (MIT), to guarantee detectable ferromagnetic resonance (FMR) absorption for the present thin (Ga,Mn)As layer. The sample is processed into a MIS structure (Fig. 1) with an Al_2O_3 gate insulator formed by atomic layer deposition at 130 °C and a Au/Cr gate electrode by thermal evaporation at ambient temperature. A positive gate voltage V_G is defined as a positive voltage applied to the metal gate with respect to (Ga,Mn)As.

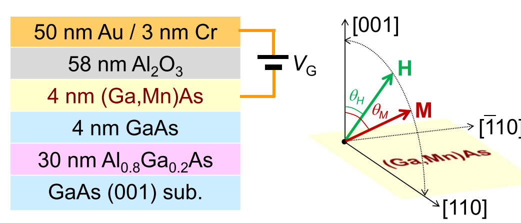

FIG. 1 (color online). Schematic of metal-insulator-semiconductor (MIS) structure for ferromagnetic resonance and magnetization measurements. Capacitance area is 1.0×2.3 mm^2. Right panel shows crystal orientations of (Ga,Mn)As and the definition of angles of magnetic field θ_H and magnetization θ_M.

The capacitance of the device is determined to be $0.27\ \mu\mathrm{F/cm}^2$ from the gate-voltage sweep rate dependence of the charge and discharge current. The maximum applied V_G is 24 V, which corresponds to an electric field of $\sim$4 MV/cm. Hole concentration p is modulated by $\sim$25% from $2.8\times10^{20}\ \mathrm{cm}^{-3}$ at $+24$ V to $3.5\times10^{20}\ \mathrm{cm}^{-3}$ at -24 V, where p is determined from the gate-voltage dependence of the sheet conductance by assuming the gate-voltage independent carrier mobility [17,30].

Figures 2(a) presents FMR spectra at $V_G = 0$ as a function of the magnetic-field angle θ_H, measured at microwave frequency $f = 9.0$ GHz (its power $P = 3$ mW) at 15 K. The angle θ_H and magnetization angle θ_M are measured from the device normal, as shown in Fig. 1. We obtain resonant field H_R and linewidth ΔH, which correspond to the center field between peak and dip fields and $3^{1/2}$ times peak-to-dip width [31], by averaging the values determined from 5 measurements of each spectrum with $\sim$0.01 mT steps. Figures 2(b) and 2(c) present the FMR spectra at 20 K as a function of V_G at $\theta_H = 0°$ and 90°, where the modulation of the spectra is clearly observed. The gate-voltage dependence of H_R and ΔH is summarized in Figs. 2(d)–2(g) with error bars representing their variations over 5 measurements. The dependence of H_R at $\theta_H = 0°$ and 90° shows the opposite tendency; i.e., $\mu_0 H_R$ (μ_0 is permeability in vacuum) decreases by $\sim$1 mT at $\theta_H = 0°$ [Fig. 2(d)], while it increases by $\sim$1 mT at $\theta_H = 90°$ [Fig. 2(e)] by changing V_G from -23 V to $+24$ V. This results from the change of the magnetic anisotropy field under V_G through the change of p as well as magnetization [32]. The magnitude of $\mu_0\Delta H$ increases by $\sim$4 mT with increasing V_G for both angles [Figs. 2(f) and 2(g)]. We measure the gate-voltage dependence of FMR spectra of three other devices with a 4-nm (Ga,Mn)As channel for the same x of 0.13 or different x of 0.11, and observe similar behavior with the modulation of the linewidth by 5%–10%.

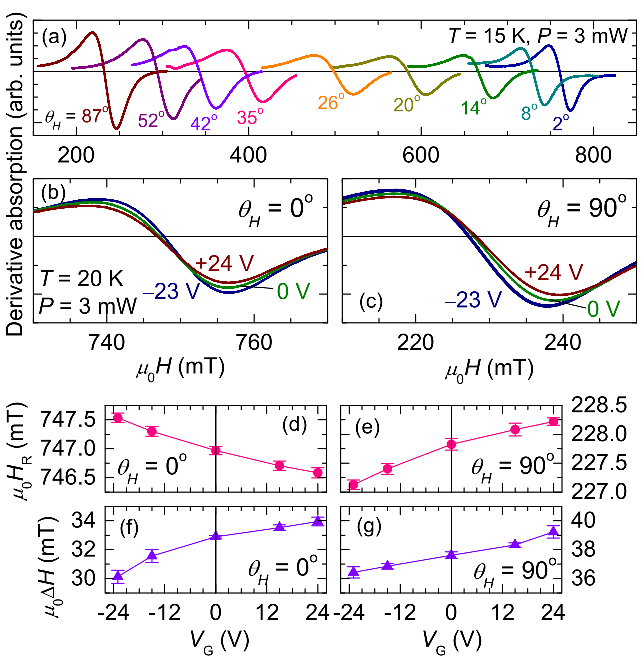

FIG. 2 (color online). Ferromagnetic resonance spectra as a function of (a) magnetic-field angle θ_H at 15 K, and as a function of gate voltages V_G at 20 K at magnetic-field angles (b) $\theta_H = 0°$ and (c) $\theta_H = 90°$. Gate-voltage V_G dependence of resonant fields H_R at (d) $\theta_H = 0°$ and (e) $\theta_H = 90°$ and that of linewidths ΔH at (f) $\theta_H = 0°$ and (g) $\theta_H = 90°$.

Figure 3(a) presents the magnetic-field angle dependence of H_R at V_G of -23, 0, and $+24$ V, where the modulation of H_R is almost invisible due to the scale of the figure. The dependence is fitted by the resonant condition [33],

$$\left(\frac{\omega}{\gamma}\right)^2 = \mu_0^2 H_1 H_2, \tag{1}$$

with

$$H_1 = H\cos(\theta_H - \theta_M) + \left(-H_K - H_{\mathrm{U}} - \frac{H_B}{4}\right)\cos 2\theta_M + \frac{H_B}{4}\cos 4\theta_M, \tag{2}$$

and

$$H_2 = H\cos(\theta_H - \theta_M) + \left(-H_K - H_U + \frac{H_B}{2}\right)\cos^2\theta_M + \frac{H_{\mathrm{B}}}{2}\cos^4\theta_M - H_B + H_U, \tag{3}$$

for the configuration shown in Fig. 1. Here, ω is the angular frequency of magnetization precession ($\omega = 2\pi f$), γ the gyromagnetic ratio ($\gamma = g\mu_B/\hbar$), g the Landé g factor, μ_B the Bohr magneton, $\hbar$ the Dirac constant, H_K the effective perpendicular magnetic anisotropy field including

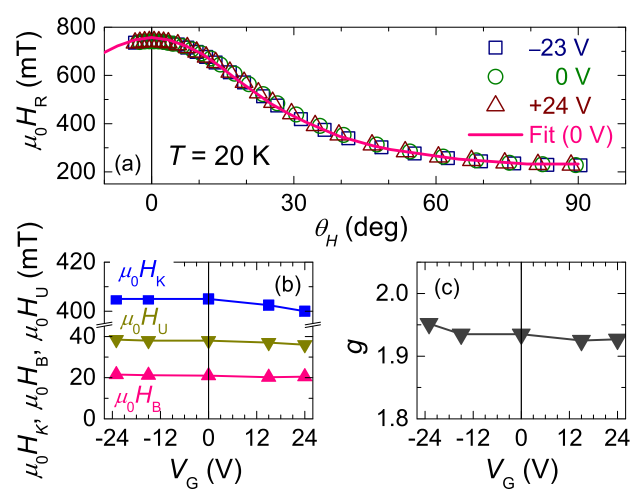

FIG. 3 (color online). (a) Magnetic-field angle dependence of resonant fields H_R at 20 K as a function of gate voltages V_G. Symbols represent experimental results, and the solid line is the fit by Eq. (1). Gate-voltage dependence of (b) magnetic anisotropy fields, H_K, H_B, and H_U, and (c) Landé g factor g.

demagnetizing field, H_B the in-plane biaxial magnetic anisotropy field along $\langle 100 \rangle$, and H_U the in-plane uniaxial magnetic anisotropy field along the $[\bar{1}10]$ orientation [34]. Figures 3(b) and 3(c) summarize the gate-voltage dependence of the magnetic anisotropy fields and g factor. The modulation of the magnetic anisotropy fields is small as noticed from small modulation of H_R [Figs. 2(d) and 2(e)]. The obtained g value is ~ 1.95, slightly smaller than 2, which is expected to result from the antiferromagnetic coupling between localized Mn^{2+} and holes [33,35]. The almost constant g is consistent with the previous study on (Ga,Mn)As with p ranging from 10^{19} cm^{-3} to 10^{21} cm^{-3} [36].

For other magnetic materials, it is known that extrinsic effects, such as inhomogeneity and two-magnon scattering, contribute very often to FMR linewidth broadening [13,31,37,38]. For (Ga,Mn)As, however, it was shown that the magnetic-field angle dependence of ΔH can be described solely by considering the isotropic damping constant [39]. Figure 4(a) shows the magnetic-field angle dependence of ΔH as a function of V_G, where clear modulation of ΔH is seen. The dependence is fitted by calculating the linewidth of the imaginary part of dynamic susceptibility χ'', which is proportional to the FMR absorption. The expression for χ'' is obtained by solving the Landau-Lifshitz-Gilbert (LLG) equation as

$$\chi'' = \frac{\alpha\sqrt{H_1^R H_2^R}[H_1(H_1+H_2)+(H_1^R H_2^R - H_1 H_2)]}{(H_1 H_2 - H_1^R H_2^R)^2 + \alpha^2 H_1^R H_2^R (H_1+H_2)^2} M, \tag{4}$$

where $H_1{}^R$ and $H_2{}^R$ are H_1 and H_2 at H_R, and M the magnetization [39]. As shown by solid lines in Fig. 4(a), the magnetic-field angle dependence of ΔH can be reproduced by using Eq. (4) with α as an adjustable parameter and magnetic anisotropy fields in Fig. 3(b). The modulation of the amplitudes of the FMR signals observed in Figs. 2(b) and 2(c) is also described by Eq. (4) through the modulation of the magnetic anisotropy and α (not shown). Figure 4(b) shows the gate-voltage dependence of α, which is modulated by $\sim 10\%$ from 0.0523 at -23 V to 0.0578 at $+24$ V.

Now, we discuss the mechanism of the modulation of α. For metal ferromagnets, α is known to often scale with the magnitude of magnetic anisotropy field and/or $(g-2)^2$ [40,41]. This is reasonable because the spin-orbit coupling determines the magnitudes of α, magnetic anisotropy, and the deviation of g from 2 [42]. Our experimental finding, however, is that the modulation of α is sizable, while those of the magnetic anisotropy fields and g factor are small. The intrinsic damping constant related to the spin-orbit coupling is known to be determined by the combined effects of intra- and interband transitions [6,43]. The contribution from the intraband transition results in α inversely proportional to the electron scattering rate and thus inversely proportional to the electrical resistivity ρ, $\alpha_{\mathrm{intra}} \propto 1/\rho$. On the other hand, the contribution from the interband transition results in α proportional to the scattering rate and thus to ρ, $\alpha_{\mathrm{inter}} \propto \rho$ [43]. For (Ga,Mn)As, the contributions from both transitions are expected due to the spin mixing resulting from the spin-orbit coupling in the valence band. α is also shown to depend on the magnitude of the p-d exchange coupling, because it affects the degree of spin mixing [44]. This model predicts that α increases with increasing p for metallic (Ga,Mn)As through the increase of the density of states at the Fermi level [44,45]. The present observation, however, reveals an opposite trend to this theoretical expectation, but seems to be consistent with the interband transition mechanism. To check if this is the case, we measure the temperature dependence of ρ as a function of V_G in a field-effect structure with a Hall-bar geometry from the same wafer. As shown in Fig. 5(a), ρ increases by $\sim 25\%$ by changing V_G from -24 V to $+24$ V, which is much larger than the modulation of α of $\sim 10\%$. This suggests that α in (Ga,Mn)As is determined not by the interband transition or at least not by the interband transition alone.

Because (Ga,Mn)As is in the vicinity of the MIT even for metallic samples and its ferromagnetism is mediated by holes, there exists magnetic disorder due to local fluctuation of the hole concentration in (Ga,Mn)As with uniform Mn distribution and flat interfaces [19,46–48]. The region richly populated by holes shows ferromagnetic response, whereas that poorly populated by holes shows superparamagneticlike response [19]. For a MIS structure, the ratio of the two regions is modulated by the application of V_G through the change of hole distribution in (Ga,Mn)As

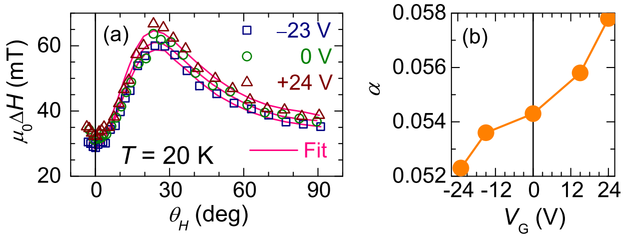

FIG. 4 (color online). (a) Magnetic-field angle dependence of linewidths ΔH at 20 K as a function of gate voltages V_G. Symbols represent experimental results, and solid lines are fittings by using Eq. (4). (b) Gate-voltage dependence of damping constants α.

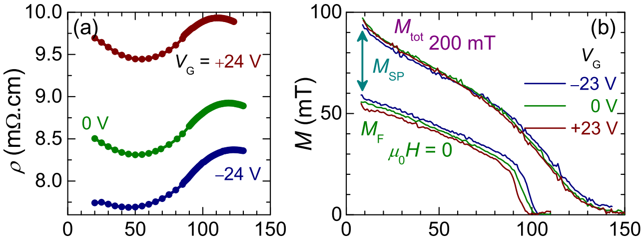

FIG. 5 (color online). (a) Temperature dependence of resistivity ρ at gate voltages V_G of -24, 0, and $+24$ V. (b) Temperature dependence of in-plane magnetization M for zero-field cooled state and state under magnetic field $\mu_0 H$ of 200 mT at gate voltages V_G of -23, 0, and $+23$ V. T_C is modulated by ~ 6 K.

near the interface with a gate insulator [19]. As shown in Fig. 5(b), we determine the magnetization components, M_F and $M_{\rm SP}$, corresponding to ferromagnetic and superparamagneticlike responses, respectively, by measuring the temperature dependence of magnetization. The M_F is detected as magnetization at zero magnetic field in the zero-magnetic-field cooled state [19]. The sum $M_{\rm tot}$ of M_F and $M_{\rm SP}$, is detected as the magnetization under a magnetic field of 200 mT larger than saturation field, where $M_{\rm SP}$ (the difference between $M_{\rm tot}$ and M_F) includes blocked and unblocked superparamagneticlike components. The M_F decreases under positive V_G due to the increase of the depletion thickness, while $M_{\rm tot}$ is almost independent of V_G. The gate-voltage independent $M_{\rm tot}$ shows that the portion of M_F is converted to the component of $M_{\rm SP}$ through, for example, the formation of ferromagnetic clusters or bound magnetic polarons (BMPs). Because the Bohr radius of Mn is ~1 nm [49], one Mn ion contacts with a few tens of other Mn ions for (Ga,Mn)As with effective Mn composition of 0.075 to form BMPs in the depleted regime. The ratio of $M_{\rm SP}/M_{\rm tot}$, which is a measure of the degree of the magnetic disorder, increases with increasing ρ. To investigate the effect of the disorder in a wider range of ρ, we grow a 200-nm-thick insulating pseudomorphic (Ga,Mn)As layer ($x = 0.075$) and a 20-nm-thick layer with metallic conductivity ($x = 0.068$) through a GaAs buffer layer on a GaAs substrate in the same MBE chamber used for the MIS sample. Because the FMR intensity is determined by the total magnetic moments and conductivities of the sample, one needs a thicker layer of (Ga,Mn)As with less x and/or conductivity. The samples are annealed at several different conditions with annealing temperature between 200 °C and 250 °C and annealing time up to 45 min [50], to investigate the resistivity dependence of magnetization and α of (Ga,Mn)As. The ratio of $M_{\rm SP}/M_{\rm tot}$ is larger in samples with higher resistivity, as shown in Figs. 6(a) and 6(b). We also measure FMR spectra as a function of θ_H to determine α for these samples. For samples with large $M_{\rm SP}/M_{\rm tot}$, the FMR signal survives slightly above T_C, and both H_R and ΔH vary continuously across T_C, while the FMR signal disappears at T_C for samples with small $M_{\rm SP}/M_{\rm tot}$. This suggests that ferromagnetic and superparamagneticlike components are detected simultaneously by FMR. The closed symbols in Fig. 6(c) show α as a function of ρ, which shows a very similar trend to $M_{\rm SP}/M_{\rm tot}$ (open symbols). The squares present $M_{\rm SP}/M_{\rm tot}$ and α for the MIS devices as a function of ρ, where ρ is changed by the applied V_G. A similar resistivity dependence of α and $M_{\rm SP}/M_{\rm tot}$ is again obtained. Figure 6(d) replots α in its $M_{\rm SP}/M_{\rm tot}$ dependence, which shows the curves for all the samples with different ρ coalesce into a single curve. This observation suggests strongly that α in (Ga,Mn)As is determined mainly by the magnetic disorder induced by carrier localization. The result also confirms that the application of V_G changes the degree of the disorder in the MIS structure, and thus

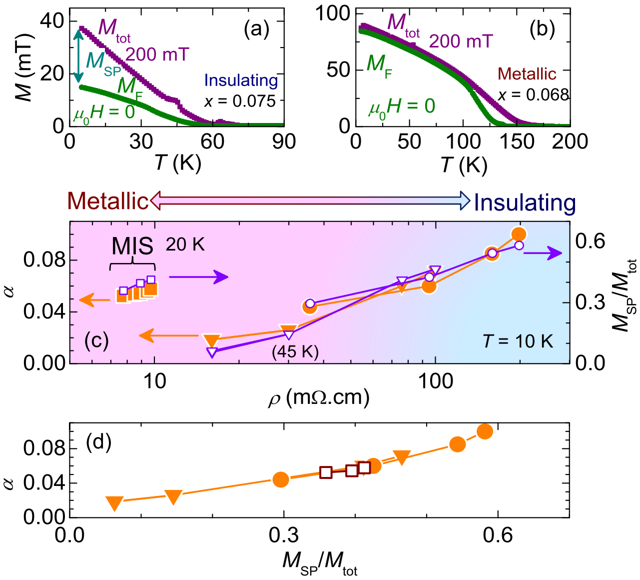

FIG. 6 (color online). Temperature dependence of magnetization M of zero-field cooled state and state under magnetic field $\mu_0 H = 200$ mT for (a) a 200-nm-thick insulating sample with $x = 0.075$ and (b) a 20-nm-thick metallic sample with $x = 0.068$. (c) Damping constant α (closed symbols) and ratio of superparamagneticlike component $M_{\rm SP}$ to total magnetic component $M_{\rm tot}$ (open symbols) as a function of resistivity ρ. Circles (triangles) are for the sample with $x = 0.075$ (0.068), whose ρ is changed by annealing. Squares are for the MIS structure, whose ρ is change by applied gate voltage. The results for the samples with $x = 0.075$ and 0.068 are taken at 10 K except for one α value obtained at 45 K as indicated, and those for the MIS structure are taken at 20 K. (d) α as a function of $M_{\rm SP}/M_{\rm tot}$. Circles and triangles are for (Ga,Mn)As with $x = 0.075$ and 0.068, respectively. Squares are for (Ga,Mn)As in the MIS structure.

modulates the magnitude of α. Other possible effects on α, such as magnetoelastic effect through piezoelectric effect, seem to be less effective.

In summary, we demonstrate the modulation of damping constant α of (Ga,Mn)As by the application of gate voltages. A relatively large modulation ratio of ~10% is observed, whereas the modulation ratios of other magnetic constants, such as saturation magnetization, magnetic anisotropy fields, and Landé g factor, are much smaller. The modulation of α results from the modulation of the ratio of superparamagneticlike to the total magnetic component, indicating that the degree of magnetic disorder related to the metal-insulator transition plays a major role in determining α in (Ga,Mn)As. The results are important for further understanding of the microscopic origin of α, as well as for developing an efficient way to control the magnitude of α.

The authors thank T. Dietl, T. Jungwirth, J. Sinova, I. Garate, and D. Chiba for useful discussions, as well as S. Kanai and S. D'Ambrosio for their technical help. This work was supported in part by a Grants-in-Aid for Scientific Research (B) (No. 23360002) and for Scientific Research on

Innovative Areas (No. 26103002), the ASPIMATT program from JST, "Funding program world-leading innovative R&D on Science and Technology (FIRST program)"of JSPS, and R&D Project for ICT Key Technology of MEXT.

*Corresponding author.
f-matsu@wpi-aimr.tohoku.ac.jp

[1] T. L. Gilbert, IEEE Trans. Magn. **40**, 3443 (2004).
[2] J. C. Slonczewski, J. Magn. Magn. Mater. **159**, L1 (1996).
[3] L. Berger, Phys. Rev. B **54**, 9353 (1996).
[4] S. Mizukami, F. Wu, A. Sakuma, J. Walowski, D. Watanabe, T. Kubota, X. Zhang, H. Naganuma, M. Oogane, Y. Ando, and T. Miyazaki, Phys. Rev. Lett. **106**, 117201 (2011).
[5] S. Mizukami, S. Iihama, N. Inami, T. Hiratsuka, G. Kim, H. Naganuma, M. Oogane, and Y. Ando, Appl. Phys. Lett. **98**, 052501 (2011).
[6] V. Kamberský, Czech. J. Phys. B **26**, 1366 (1976).
[7] Y. Tserkovnyak, A. Brataas, and G. E. W. Bauer, Phys. Rev. Lett. **88**, 117601 (2002).
[8] S. Mizukami, Y. Ando, and T. Miyazaki, Phys. Rev. B **66**, 104413 (2002).
[9] P. He, X. Ma, J. W. Zhang, H. B. Zhao, G. Lüpke, Z. Shi, and S. M. Zhou, Phys. Rev. Lett. **110**, 077203 (2013).
[10] A. A. Starikov, P. J. Kelly, A. Brataas, Y. Tserkovnyak, and G. E. W. Bauer, Phys. Rev. Lett. **105**, 236601 (2010).
[11] M. Oogane, T. Kubota, Y. Kota, S. Mizukami, H. Naganuma, A. Sakuma, and Y. Ando, Appl. Phys. Lett. **96**, 252501 (2010).
[12] A. Barman, S. Wang, J. Maas, A. R. Hawkins, S. Kwon, J. Bokor, A. Liddle, and H. Schmidt, Appl. Phys. Lett. **90**, 202504 (2007).
[13] A. Okada, S. Kanai, M. Yamanouchi, S. Ikeda, F. Matsukura, and H. Ohno, Appl. Phys. Lett. **105**, 052415 (2014).
[14] H. Ohno, D. Chiba, F. Matsukura, T. Omiya, E. Abe, T. Dietl, Y. Ohno, and K. Ohtani, Nature (London) **408**, 944 (2000).
[15] D. Chiba, M. Yamanouchi, F. Matsukura, and H. Ohno, Science **301**, 943 (2003).
[16] D. Chiba, F. Matsukura, and H. Ohno, Appl. Phys. Lett. **89**, 162505 (2006).
[17] D. Chiba, M. Sawicki, Y. Nishitani, Y. Nakatani, F. Matsukura, and H. Ohno, Nature (London) **455**, 515 (2008).
[18] M. H. S. Owen, J. Wunderlich, V. Novák, K. Olejník, J. Zemen, K. Výborný, S. Ogawa, A. C. Irvine, A. J. Ferguson, H. Sirringhaus, and T. Jungwirth, New J. Phys. **11**, 023008 (2009).
[19] M. Sawicki, D. Chiba, A. Korbecka, Y. Nishitani, J. A. Majewski, F. Matsukura, T. Dietl, and H. Ohno, Nat. Phys. **6**, 22 (2010).
[20] F. X. Xiu, Y. Wang, J. Y. Kim, A. Hong, J. S. Tang, A. P. Jacob, J. Zou, and K. L. Wang, Nat. Mater. **9**, 337 (2010).
[21] Y. Yamada, K. Ueno, T. Fukumura, H. T. Yuan, H. Shimotani, Y. Iwasa, L. Gu, S. Tsukimoto, Y. Ikuhara, and M. Kawasaki, Science **332**, 1065 (2011).
[22] M. Weisheit, S. Fähler, A. Marty, Y. Souche, C. Poinsignon, and D. Givord, Science **315**, 349 (2007).
[23] T. Maruyama, Y. Shiota, T. Nozaki, K. Ohta, N. Toda, M. Mizuguchi, A. A. Tulapurkar, T. Shinjo, M. Shiraishi, S. Mizukami, Y. Ando, and Y. Suzuki, Nat. Nanotechnol. **4**, 158 (2009).
[24] M. Endo, S. Kanai, S. Ikeda, F. Matsukura, and H. Ohno, Appl. Phys. Lett. **96**, 212503 (2010).
[25] D. Chiba, S. Fukami, K. Shimanura, N. Ishiwata, K. Kobayashi, and T. Ono, Nat. Mater. **10**, 853 (2011).
[26] Y. Shiota, T. Nozaki, F. Bonell, S. Murakami, T. Shinjo, and Y. Suzuki, Nat. Mater. **11**, 39 (2012).
[27] S. Kanai, M. Yamanouchi, S. Ikeda, Y. Nakatani, F. Matsukura, and H. Ohno, Appl. Phys. Lett. **101**, 122403 (2012).
[28] H. Ohno, A. Shen, F. Matsukura, A. Oiwa, A. Endo, S. Katsumoto, and Y. Iye, Appl. Phys. Lett. **69**, 363 (1996).
[29] K. Y. Wang, K. W. Edmonds, R. P. Campion, B. L. Gallagher, N. R. S. Farley, C. T. Foxon, M. Sawicki, P. Boguslawski, and T. Dietl, J. Appl. Phys. **95**, 6512 (2004).
[30] Y. Nishitani, D. Chiba, M. Endo, M. Sawicki, F. Matsukura, T. Dietl, and H. Ohno, Phys. Rev. B **81**, 045208 (2010).
[31] S. Mizukami, Y. Ando, and T. Miyazaki, Jpn. J. Appl. Phys. **40**, 580 (2001).
[32] T. Dietl, H. Ohno, and F. Matsukura, Phys. Rev. B **63**, 195205 (2001).
[33] X. Liu and J. K. Furdyna, J. Phys. Condens. Matter **18**, R245 (2006).
[34] U. Welp, V. K. Vlasko-Vlasov, X. Liu, J. K. Furdyna, and T. Wojtowicz, Phys. Rev. Lett. **90**, 167206 (2003).
[35] C. Śliwa and T. Dietl, Phys. Rev. B **74**, 245215 (2006).
[36] Kh. Khazen, H. J. von Bardeleben, J. L. Cantin, L. Thevenard, L. Largeau, O. Mauguin, and A. Lemaître, Phys. Rev. B **77**, 165204 (2008).
[37] R. Arias and D. L. Mills, Phys. Rev. B **60**, 7395 (1999).
[38] Kh. Zakeri, J. Lindner, I. Barsukov, R. Meckenstock, M. Farle, U. von Hörsten, H. Wende, W. Keune, J. Rocker, S. S. Kalarickal, K. Lenz, W. Kuch, K. Baberschke, and Z. Frait, Phys. Rev. B **76**, 104416 (2007).
[39] L. Chen, F. Matsukura, and H. Ohno, Nat. Commun. **4**, 2055 (2013).
[40] S. Pal, B. Rana, O. Hellwig, T. Thomson, and A. Barman, Appl. Phys. Lett. **98**, 082501 (2011).
[41] M. Oogane, T. Wakitani, S. Yakata, R. Yilgin, Y. Ando, A. Sakuma, and T. Miyazaki, Jpn. J. Appl. Phys. **45**, 3889 (2006).
[42] V. Kamberský, Phys. Rev. B **76**, 134416 (2007).
[43] I. Garate and A. H. MacDonald, Phys. Rev. B **79**, 064404 (2009).
[44] J. Sinova, T. Jungwirth, X. Liu, Y. Sasaki, J. K. Furdyna, W. A. Atkinson, and A. H. MacDonald, Phys. Rev. B **69**, 085209 (2004).
[45] K. Shen and M. W. Wu, Phys. Rev. B **85**, 075206 (2012).
[46] F. Matsukura, M. Sawicki, T. Dietl, D. Chiba, and H. Ohno, Physica (Amsterdam) **21E**, 1032 (2004).
[47] T. Dietl, J. Phys. Soc. Jpn. **77**, 031005 (2008).
[48] M. Kodzuka, T. Ohkubo, K. Hono, F. Matsukura, and H. Ohno, Ultramicroscopy **109**, 644 (2009).
[49] M. Berciu and R. N. Bhatt, Phys. Rev. Lett. **87**, 107203 (2001).
[50] K. W. Edmonds, P. Bogusławski, K. Y. Wang, R. P. Campion, S. N. Novikov, N. R. S. Farley, B. L. Gallagher, C. T. Foxon, M. Sawicki, T. Dietl, M. Buongiorno Nardelli, and J. Bernholc, Phys. Rev. Lett. **92**, 037201 (2004).